A duality-based model of the controlled shunt compensator of transformer type (CSCT)

Mohammad Tavakoli Bina *, Hosein Samsami, Hamed Valizadeh Haghi

Faculty of Electrical and Computer Engineering, K.N. Toosi University of Technology, P.O. Box: 16315-1355, Tehran, Iran

ARTICLE INFO

ABSTRACT

This paper discusses the structure of controlled shunt compensator of transformer type (CSCT) based on its operating principles. The modeling procedure of CSCT is further explored from a duality-based modeling viewpoint. Then, an experimental prototype is implemented and the results are measured up to the theory and simulation. Finally, the proposed model is used to simulate the interchanged reactive power between network and CSCT in order to demonstrate the capabilities of this compensator in both capacitive and inductive modes of operation.

© 2013 Elsevier Ltd. All rights reserved.

1. Introduction

Transmission lines are bulky reactive power sources and often operate with surplus reactive power. This gives rise to several problems [1]; as a result, using reactive power compensation is indispensable. There is a variety of compensation techniques, controllers and devices, such as synchronous condensers, conventional shunt reactors, static VAR compensators (SVCs) and controllable reactors are developed to cater for such demand. By now, synchronous condensers nearly have been abandoned. Conventional shunt reactors cannot provide smooth power regulation, hence, cannot satisfy the requirements of excessively-high voltage long-distance networks. Owing to their complicated techniques, high manufacture cost and difficult maintenance, SVC are inapplicable for some countries which has lower semiconductor technique and economy level [2]. Hence, experts put up with some new kinds of controllable reactors such as thyristor controlled reactor (TCR), also called the controllable reactors of transformer type (CRT) [3], and the magnetic controllable reactor (MCR) [4].

A MCR is developed on the principle of a magnetic magnifier. By controlling the angle of thyristor opening, the dc flux component in the core is regulated and thus the saturation of the core. By this means the purpose of automatic control of reactive power is realized. Unfortunately, there are two shortages inherent in MCRs [3]. First, due to the iron saturation, there is a high level of harmonics in the working currents. Then, the existence of the dc bias magnetization gives rise to large electromagnetic Inertia, which results in

low response. To get around the main defect of the MCRs, researchers proposed CRTs in the late 20th century [3].

A CRT is equivalent to a multi-winding transformer with a network winding (NW) which is connected to the network high voltage bus, and several control windings (CWs), in which a thyristor valve (TV) in parallel with a voltage circuit breaker, are connected across each of them. By controlling the TVs properly, CRT can realize the function of smooth stepwise power regulation from no load to nominal conditions, satisfying the current harmonic content constraints. In addition to those advantages of ordinary reactors, a CRT possesses other virtues such as low current harmonic content, fast response, and small losses. Therefore, a CRT can be employed to control reactive power of transmission networks [3]. However, in case there is strong inductive coupling among CWs, such negligence cannot render satisfactory results. It is noticed that the voltage of the network winding is the high voltage of the grid. Hence, when the short-circuited impedance between the NW and CW is less than 100%, current-limiting reactors (CLRs) are needed to limit the currents within the rated. When the regulation step number is more than two, the number of the windings for a CRT is larger than three. In this case, a precise calculation is very hard to obtain.

This paper presents a controlled shunt compensator of transformer type (CSCT) as a new kind of the CRTs, with only one control winding and too high short circuit reactance to solve the above problems. It provides sufficient response rate, very low total harmonic distortion (THD) and independently bidirectional reactive power injection.

The controlled shunt compensator of transformer type (CSCT) is a new compensator which can be installed in high voltage

---

transmission lines. As a controlled reactor, it provides sufficient response rate, very low total harmonic distortion (THD) and independently bidirectional reactive power injection.

The general structure of this compensator is presented in Fig. 1. The transformer consists of three windings; the network winding (NW), the control winding (CW) and the compensating winding (ComW). The NW is the main winding of the compensator and connected to the high voltage bus of the network. The CW is the second winding in which thyristor valves (TV) in parallel with a voltage circuit breaker (VCB) are connected across the secondary. The ComW, indicated as the tertiary winding in Fig. 1, includes two tuned harmonic filters connected across it. It is important to note that the CSCT is a three phase compensator. Both the NW and CW is of star-connected type with the grounded neutral. However, the ComW can be of delta-connected type.

When the TV is open, the entire magnetic flux passes through the magnetic core, leading to a minimum reluctance and maximum capacitive current in NW. This eventually injects reactive power to the network. On the other hand, with the TV closed, the flux passes through the air gap as well as the windings. Hence, the reluctance and inductive current of NW is maximal. As the latter lead to a different direction of reactive power flow, the compensator can practically operates in both capacitive and inductive modes.

Employing thyristors results in higher harmonics in the current of CSCT. Hence, a tertiary winding connected to a filtering block is required to suppress the harmonics. This includes several parallel branches, each composed of an inductor and a capacitor in series, so that each branch can bypass a certain harmonic order. In this way, the harmonic cannot pass through the main winding which is connected to the network [4].

Like other new equipment, an accurate modeling of CSCT is required prior to analyzing its behavior. This paper presents a model based on a magnetic circuit modeling framework using the principle of duality [5,6]. The steps toward building such a model and determining its parameters are given in Sections 2 and 3, respectively. Section 4 discusses model verification and experiments followed by the simulation of CSCT behavior in Section 5. Finally, conclusions are presented in Section 6.
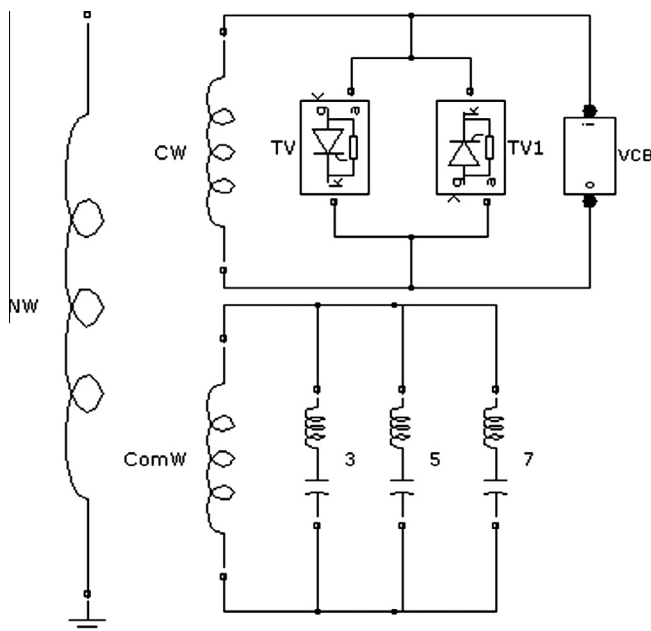
2. Modeling approach

There are a variety of approaches for transformer modeling, each of which has benefits of its own. Most of the common low-frequency models are usually based on the principle of duality [7]. Modeling CSCT based on this principle is presented in this section.

2.1. Equivalent magnetical circuit

In the equivalent magnetic circuit, windings appear as magnetomotive force (mmf) sources, leakage paths appear as linear reluctances and magnetic cores appear as saturable reluctances [8]. The magnetic equivalent circuit of CSCT is shown in Fig. 2.

The model of Fig. 2 consists of.

R_L: The reluctance of the core limb which the three windings of the phase are located on it.
R_Y: The reluctance of the yoke.
R_S: The reluctance of the magnetic shunt which covers three windings of the phase.
R_{LY}: The reluctance of lateral yokes.
R_{12}: The leakage reluctance of the air gap between the innermost winding and the middle winding of the phase.
R_{23}: The leakage reluctance of the air gap between the outmost winding and the middle winding of the phase.
F_{NW}: Magneto motive force of the network winding.
F_{CW}: Magneto motive force of the control winding.
$F_{Com.W}$: Magneto motive force of the compensating winding.

2.2. Equivalent virtual circuit

In this step, the mmf of each winding is represented by an equivalent voltage source. Also, the permeance of each magnetic path should be modeled by a capacitance of the same value. The virtual equivalent circuit of the system of Fig. 2 is shown in Fig. 3. In this figure, the permeance of limbs and yokes are modeled with nonlinear capacitances. This represents the nonlinear nature of iron core. This figure also contains some linear capacitances which represent the air gap in parallel to each limb. This is necessary due to the five-legged structure of the magnetic core.

2.3. Equivalent electrical circuit

The equivalent electrical circuit is derived from the circuit shown in Fig. 3 by using the duality concept according to following rules:

– Dual of each mesh is a node. This is true about the outer loop as well.
– Dual of the each capacitance between two meshes is an inductance between their dual nodes by the same value.
– Dual of each voltage source is a current source by the same value.

2.4. Final model

The final model of the CSCT is obtained by adding/replacing the following elements as shown in Fig. 4 [8]:

– The duals of current sources are replaced with ideal transformers assuming only one turn on the secondary for which the primary turn is determined such that the turns ratio equals to in the related winding of CSCT.
– Add a resistance in parallel with each core inductance to represent the magnetic core losses in limb, yoke or lateral yoke.

Fig. 1. General scheme of CSCT: TV-thyristor valve, VCB: vacuum circuit breaker, 3, 5 and 7: filter of third, fifth and seventh harmonics.
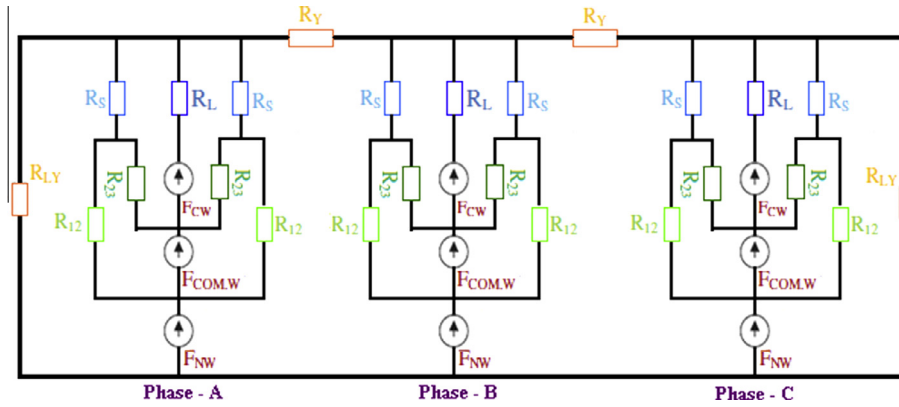
Fig. 2. Equivalent magnetic circuit of CSCT.
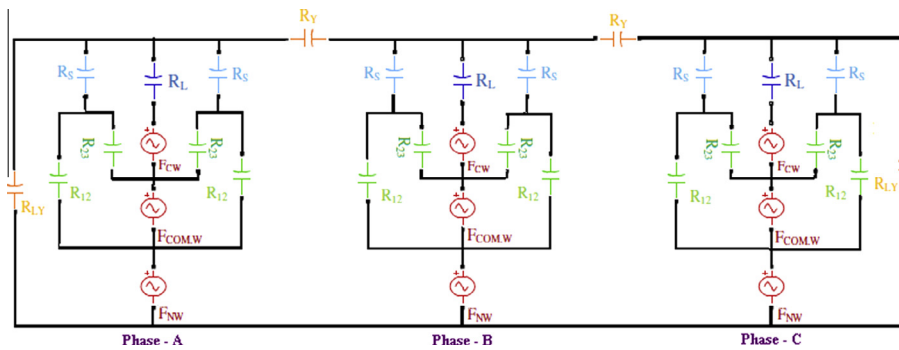
Fig. 3. Equivalent virtual circuit of CSCT.

– Add a series resistance to each ideal transformer to model the winding losses.

Following parameters are used in Fig. 4:

L_L: The inductance of the core limb along with three windings of the phase.
R_L: The resistance representing losses of the core limb along with three windings of the phase.
L_Y: The inductance of the yoke.
R_Y: The resistance representing losses of the yoke.
L_S: The inductance of the magnetic shunt branch along with the three windings of the phase.
R_S: The resistance representing losses of the magnetic shunt.
L_{LY}: The inductance of the lateral yoke.
R_{LY}: The resistance representing losses of the lateral yoke.
L_1: The leakage inductance of the air gap between the outermost winding and the middle winding.
L_2: The leakage inductance of the air gap between the innermost winding and the middle winding.
L_3: The leakage inductance resulted from the mutual effect between the inductances L_1 and L_2.
R_{NW}: The resistance of the network winding.
R_{CW}: The resistance of the control winding.
R_{NW}: The resistance of the compensating winding.

Some points should be mentioned regarding the model of Fig. 4. First, it is important to note that, unlike other duality-based models of transformers, this model is symmetric. In fact, previous models allow for one path of leakage flux between the windings [9,10]; whereas, the proposed equivalent magnetic circuit of CSCT, as shown in Fig. 3, allocates two paths to the leakage flux. Second,

the proposed model is generally more accurate than other duality-based models. This needs to be confirmed by comparing experimental and simulation results. As a first point in view, it is shown that the most important feature of duality-based models is their capability in modeling nonlinear behaviors of magnetic core. On the other hand, these models have significant errors considering short circuit tests [7]. In order to solve this problem, STC models of three-winding transformers [7] consist of three subsidiary inductances connected between three leakage inductances L_1, L_2 and L_3. Hence, the proposed duality-based model of CSCT uses such a subsidiary set of inductances in addition to the leakage inductances L_1 and L_2. As a result, the CSCT model of Fig. 4 is a hybrid model using duality principles to represent the magnetic core as well as the STC method to represent the windings.

3. Parameter estimation

Methods to estimate the parameters of the proposed CSCT model are presented in this section. Parameters can be estimated from test measurements and/or physical structure of the transformer. This work uses a combination of measurement and calculation to determine the parameters of CSCT model as shown in Fig. 4.

3.1. Core inductance

The duality-based models represent the magnetic core by an inductance, according to (1)–(4):

$$N \cdot I = \Re \cdot \Phi \tag{1}$$

$$N \cdot \frac{\partial I}{\partial t} = \Re \cdot \frac{\partial \Phi}{\partial t} \tag{2}$$

Fig. 4. Duality base model of CSCT.

$$N \cdot \frac{\partial I}{\partial t} = \frac{l}{\mu A} \cdot \frac{V}{N} \tag{3}$$

$$\left(\frac{N^2 \cdot \mu \cdot A}{l} \right) \cdot \frac{\partial I}{\partial t} = V \tag{4}$$

where N is the number of the winding turns, I is the winding current, V is the winding voltage, R is the core reluctance, Φ is the core flux, μ is the core permeability, A is the core net-sectional area, and l is the length of the core.

Therefore, some of inductances can be estimated by:

$$L = \frac{N^2 \cdot \mu \cdot A}{l} \tag{5}$$

For which, considering the turns ratio of the ideal transformer in the proposed model, $N = 1$, therefore;

$$L = \frac{\mu \cdot A}{l} \tag{6}$$

Complete design information of CSCT is available including core dimensions (net cross-sectional area and lengths of legs). Therefore, estimation of the inductance requires permeability (μ). The permeability is determined by

$$\mu = \frac{\partial B}{\partial H} \tag{7}$$

where B is the magnetic flux density, and H is the magnetic field intensity.

This paper uses a new method based on some experiments and the Lagrange interpolation to confirm the behavior of μ. In this method ten core sheets were tested according to IEC 60404-3 for 36 times and the magnetic flux density and the magnetic field intensity were determined each time. Subsequently, the following equation can be obtained considering the Lagrange interpolation [11].

$$\mu(B) = \sum_{j=1}^{36} A_j \cdot (B)^{j-1} \tag{8}$$

Therefore, identification of magnetic flux density in each part of CSCT core, gives the core inductances of the model by using (8) and (6), respectively.

Fig. 5 shows the μ–B curve which is obtained by using the presented method. The core material (i.e. HIB) is known from Iran Transfo Company that provides laboratory support for implementing a CSCT.

3.2. Core resistance

The core resistance, similar to the core inductance, can be estimated by Lagrange interpolation using recorded experimental data of the core material. Hence, the obtained estimations are more accurate than those obtained using the previous theoretical methods (e.g. [12]).

In order to calculate the core resistance, the core sheet was tested 36 times; and its losses, magnetic flux density and voltage (rms) was measured each time. Then, the equivalent resistance of the core sheet could be estimated by the following equation for each test. It should be noted that all tests considered the rolling direction of the sheets.

$$R = \frac{V_{rms}^2}{P} \tag{9}$$

where R is the resistance of the core sheet, V is the test voltage, and P is the power losses of the core sheet.

Similar to the inductance estimation, ten specimens have been tested and the average value of resistances confirmed as the final value in Lagrange interpolation calculations. This would reduce the error to a minimum value. Finally, a function like (10) can be obtained representing the sheet resistance variations.
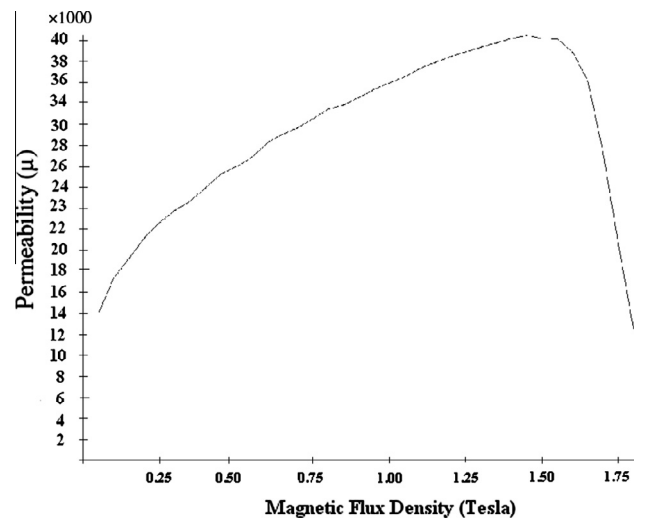
Fig. 5. Simulation of $\mu(B)$.
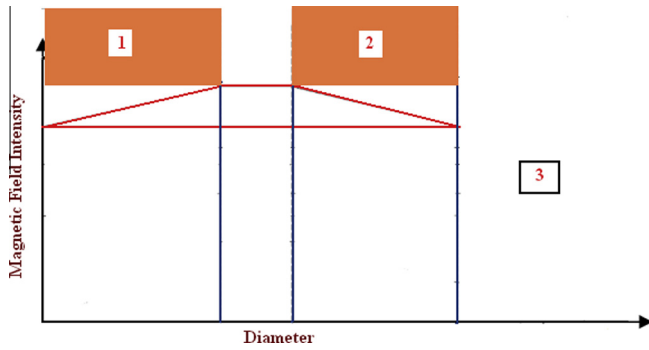
Fig. 6. Distribution of magnetic leakage field intensity in the windings where, 1: inside the inner winding, 2; between the inner and the outer winding and 3: outside of the windings.

$$R_{Sh}(B) = \sum_{j=1}^{36} C_j \cdot (B)^{j-1} \tag{10}$$

The resistances of each sections of the core (limb, yoke or lateral yoke) can be estimated by following equation:

$$R(B) = \frac{n \cdot W}{L} \cdot R_{Sh}(B) \tag{11}$$

where R is the resistance of special part of the core, B is the magnetic flux density, n is the number of the sheets in a specific section of the core, W is the width of a specific section of the core, and L is the length of a specific section of the core.

3.3. Leakage inductance

The leakage inductance can be calculated from the electromagnetic energy stored in the coils:

$$W = \frac{\mu_0}{2} \int \int_v \int H^2 \cdot dV \tag{12}$$

where W is the electromagnetic energy, H is the magnetic field intensity, and V is the volume of the coils.

On the other hand, the total leakage inductance of the winding can be calculated using the equation:

$$W = \frac{1}{2} \cdot L \cdot I^2 \tag{13}$$

where W is the electromagnetic energy, L is winding inductance, I is the winding current.

By comparing (12) with (13), the leakage inductance can be determined. Furthermore, a hypothetical short circuit analysis provides a straight forward calculation of the magnetic field intensity [13], as shown in Fig. 6 in which the hypothetical short circuit analysis is illustrated.

Based on the short circuit tests and by using the magnetic energy method [14] the leakage inductances L_1, L_2 and L_3 would be according to (14)–(16):

$$L_1 = \frac{\mu_0 \cdot \pi \cdot}{l} \cdot \left(\left(d_{NC} \cdot \left(a_{NC} + \frac{a_N + a_C}{3} \right) + \left(\frac{a_N - a_C}{3} \right) \cdot \left(a_{NC} + \frac{a_N + a_C}{2} \right) \right) \right.$$
$$+ \left(d_{NCom} \cdot \left(a_{NCom} + \frac{a_N + a_{Com}}{3} \right) + \left(\frac{a_N - a_{Com}}{3} \right) \cdot \left(a_{NCom} + \frac{a_N + a_{Com}}{2} \right) \right)$$
$$\left. - \left(d_{ComC} \cdot \left(a_{ComC} + \frac{a_{Com} + a_C}{3} \right) + \left(\frac{a_{Com} - a_C}{3} \right) \cdot \left(a_{ComC} + \frac{a_{Com} + a_C}{2} \right) \right) \right) \tag{14}$$

$$L_2 = \frac{\mu_0 \cdot \pi}{l} \cdot \left(\left(d_{NC} \cdot \left(a_{NC} + \frac{a_N + a_C}{3} \right) + \left(\frac{a_N - a_C}{3} \right) \cdot \left(a_{NC} + \frac{a_N + a_C}{2} \right) \right) \right.$$
$$- \left(d_{NCom} \cdot \left(a_{NCom} + \frac{a_N + a_{Com}}{3} \right) + \left(\frac{a_N - a_{Com}}{3} \right) \cdot \left(a_{NCom} + \frac{a_N + a_{Com}}{2} \right) \right)$$
$$\left. + \left(d_{ComC} \cdot \left(a_{ComC} + \frac{a_{Com} + a_C}{3} \right) + \left(\frac{a_{Com} - a_C}{3} \right) \cdot \left(a_{ComC} + \frac{a_{Com} + a_C}{2} \right) \right) \right) \tag{15}$$

$$L_3 = \frac{\mu_0 \cdot \pi}{l} \cdot \left(- \left(d_{NC} \cdot \left(a_{NC} + \frac{a_N + a_C}{3} \right) + \left(\frac{a_N - a_C}{3} \right) \cdot \left(a_{NC} + \frac{a_N + a_C}{2} \right) \right) \right.$$
$$+ \left(d_{NCom} \cdot \left(a_{NCom} + \frac{a_N + a_{Com}}{3} \right) + \left(\frac{a_N - a_{Com}}{3} \right) \cdot \left(a_{NCom} + \frac{a_N + a_{Com}}{2} \right) \right)$$
$$\left. + \left(d_{ComC} \cdot \left(a_{ComC} + \frac{a_{Com} + a_C}{3} \right) + \left(\frac{a_{Com} - a_C}{3} \right) \cdot \left(a_{ComC} + \frac{a_{Com} + a_C}{2} \right) \right) \right) \tag{16}$$

where d_{NC} is the average diameter of the NW and CW in sum, d_{NCom} is the average diameter of the NW and ComW in sum, $d_{Com,C}$ is the average diameter of the ComW and CW in sum, a_{NC} is the radial distance between the NW and CW, a_{NCom} is the radial distance

Table 1
The main information of the investigated transformer.

Power (MVA)	Freq (Hz)	Flux density (T)	Primary voltage (kV)	Secondary voltage (kV)	Tertiary voltage (kV)	Group
200	50	1.684	400	66	20	yNynd11

Table 2
Short circuit inductances comparison.

Supplied phase	Short circuited phase	Test result (P.U)	Simulation result (P.U)	Relative error (%)
MV	LV	0.0641	0.0617	3.8
HV	MV	0.0990	0.0951	4.3
HV	LV	0.1266	0.1238	2.2

Table 3
Exitation test results comparison.

Parameter		Test result	Simulation result	Relative error (%)
Current (A)	1st Phase	3.918	3.73	4.86
	2nd Phase	3.583	3.573	−0.28
	3rd Phase	3.243	3.114	−4.14
Losses (KW)	1st Phase	42.168	39.13	7.2
	2nd Phase	35.011	32.98	5.8
	3rd Phase	31.459	29.38	6.6
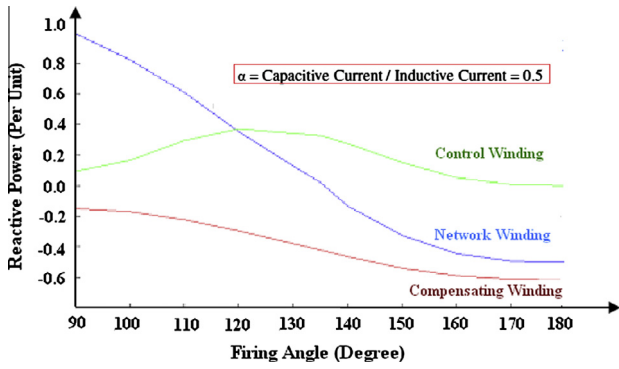
Fig. 7. Reactive power of the three windings in one phase of CSCT-NW: network winding – CW: control winding – ComW: compensating winding.
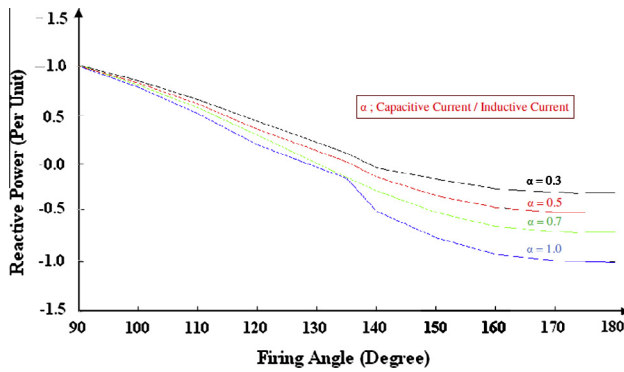
Fig. 8. Thyristor valves firing angle variation efficacy on CSCT reactive power.

Table A.1
Magnetic core dimensions.

Parameter	Value	Unit	Parameter	Value	Unit
Leg length	2404	mm	Leg section area	8536	cm^2
Yoke length	2329	mm	Yoke section area	4823	cm^2
Lateral yoke length	1517	mm	Lateral yoke section area	4823	cm^2
Leg width	1062	mm	Core diameter	1087	Mm
Yoke width	600	mm	Lateral yoke width	600	Mm

between the NW and ComW, $a_{Com,C}$ is the radial distance between the windings ComW and C, a_N is the width of the NW, a_C is width of the CW, and a_{Com} is the width of the ComW.

4. Verification

Since there is no simulation or experimental test cases in the literature that could be used for verification, we did some testing on a three phase power transformer with a structure similar to the CSCT (five-legged core with three windings).Then, the results from these tests were used to obtain the model based on the proposed methodology. Subsequently, simulations of the obtained model were compared with experiments. Table 1 lists the main data of the investigated power transformer. Furthermore, core dimensions and geometric specifications of the windings is given in appendix.

A comparison of the short circuit inductances obtained based on the proposed model and the experimental results are summarized in Table 2. The comparison shows that the inductances associated with the proposed model in the short circuit tests closely agree with the experimental results. On the other hand, Table 3 compares simulation results with the corresponding experimental results considering excitation tests. The results are verified when the same voltage is used. This proves the validity of the magnetic circuit calculation proposed in this paper. Furthermore, the error values are given based on the corresponding measured values.

5. Simulation analysis of a CSCT reactive power based on matlab/simulink

Fig. 7 shows the reactive power variations with respect to the triggering angle of the thyristor valves for each winding in one phase of CSCT. According to this figure, it is obvious that by varying the firing angle between 90° and 180°, the reactive power changes between the maximum inductive value and the maximum capacitive value. This shows the ability of the compensator to inject/absorb reactive power that would be very useful for compensating transmission lines in practice. It should be noted that the NW reactive power curve in Fig. 7 is valuable for keeping a track of reactive power exchange between the CSCT and the grid. It can be illustrated that with firing angle more than 135°, the generated reactive power by filtering block (compensating winding) is more than reactive power which network winding injects to the power system. It means that, some of the generated reactive power has been absorbed with CSCT, itself.

A remarkable characteristic of the CSCT is that the ratio of the capacitive current to the inductive current (α) can be selected according to the network conditions by the designer. For an illustration, Fig. 8 shows the reactive power variations with respect to α. This figure shows that big α, has negative affect about the CSCT inductive operation. It means that it can absorb less reactive power in compare to CSCT design with small α. On the other hand, it has positive affect about the capacitive mode operation and CSCT can inject more reactive power in this case.

The simulations show that CSCT can increases the capability of transmission lines by compensating the surplus reactive power of the line and preventing the synchronous generators to consume it leading to heat the stator edges, bears it to mind that it can be widely used in power systems.

6. Conclusion

The CSCT, as a new device to compensate reactive power in power systems, is presented in this paper. The general structure of this device and its modeling based on the duality principle is discussed. The proposed model includes equivalent inductances of the

Table A.2
Windings dimensions.

Parameter	Value	Parameter	Value
Outer winding width	188.5	Outer windings distance	84
Middle winding width	176.5	Inner windings distance	25
Inner winding width	155	Inner winding and core leg distance	19
Outer winding and upper yoke distance	205	Outer winding and lower yoke distance	95
Middle winding and upper yoke distance	181	Middle winding and lower yoke distance	71
Inner winding and upper yoke distance	176	Inner winding and lower yoke distance	66

core and magnetic paths, equivalent resistance to represent the iron losses, and the windings resistances. Experimental data is used to estimate the equivalent inductances and resistances based on Lagrange interpolation. The leakage inductances are estimated considering the electromagnetic energy stored in the coils. A three phase power transformer is used to represent the CSCT as a proto-type design benchmark. The comparison between simulations and experiments confirms a higher accuracy achieved by the proposed model.

Appendix A.

Testing Transformer Geometrical Dimensions (see Tables A.1 and A.2).

References

[1] Tavakoli Bina Mohammad, Alexandrov GN, Golkhah Mohammad. An introduction to the CSCT as a new device to compensate reactive power in electrical networks. In: Proceeding of the world congress on engineering and computer science – WCECS 2008, San Francisco, USA, Oct 22–24, 2008.
[2] Golovchan VD, Dorozhko LI. Comparison of controllable reactors and thyristor devices. Elektrotekhnika Jan. 1994;65:28–36 [in Russian].
[3] Tian Mingxing, Li Qingfu, Li Qunfeng. A controllable reactor of transformer type. IEEE Trans Power Delivery 2004;19(4):1718–26.
[4] Tavakoli Bina Mohammad, Samsami Hosein. CSCT dimensions optimization by harmony search algorithm. In: International conference on mechanical and electrical technology. ICMET 2010. September 10–12. 2010.
[5] Cherry EC. The duality between interlinked electric and magnetic circuits and the formation of transformer equivalent circuits. Proceedings of the Physical Society 1949;62B:101–11.
[6] Selmon GR. Equipment circuits for transformers and machines including non-linear effect. Proc Inst Elect Eng IV 1953;100:129–43.
[7] Martinez JuanA, Mork BruceA. Transformer modeling for low – and mid-frequency transients – a review. IEEE Trans Power Delivery 2005;20(2):1625–32.
[8] Zhalefar Farzad, Sanaye-Pasand Majid. Transformer core modeling as applied to slow transients and protective studies. IEEE 2006.
[9] Mork BA. Five-legged wound-core transformer model: derivation, parameters, implementation and evaluation. IEEE Trans Power Delivery 1999;14(4):1519–26.
[10] Garcia Sigridit, Medina Aurelio. A state space three-phase multi limb transformer model in the time domain; fast periodic steady state analysis. IEEE 2001.
[11] Wolfram S. The mathematic book. 3rd ed. Wolfram Media, Cambridge University Press; 1996.
[12] Bertotti G. General properties of power losses in soft ferromagnetic materials. IEEE Trans Magn Jan. 1988;24(1):621–30.
[13] Hayder Tammam, Scharli Ulrich, Feser Kurt. A dynamic model of transformer with tap changer using BCTRAN-Routin and 94-type. Institute of power transmission and high voltage technology (IEH). Germany: University of Stuttgart; 2008.
[14] Margueron Xavier, Jean-Pierre, Magot David. Analytical calculation of static leakage inductances of HF transformers using PEEC formulas. IEEE Trans Ind Appl 2007;43(4).